Journal of Energy and Power Engineering 8 (2014) 844-851

Simulation of FCV Fuel Consumption Using Stationary PEMFC

Yutaro Akimoto, Keiichi Okajima and Yohji Uchiyama

Department of Risk Engineering, University of Tsukuba, Tsukuba 3058573, Japan

Received: December 15, 2013 / Accepted: January 27, 2014 / Published: May 31, 2014.

Abstract: In the near future, the use of FCVs (fuel cell vehicles) is expected to help mitigate environmental problems such as exhaustion of fossil fuels and greenhouse gas emissions. Manufacturers publish an FCV's specific fuel consumption, but not its dynamic characteristics such as fuel consumption ratio and motor power ratio. Thus, it is difficult to reflect the dynamic characteristics of FCVs in lifecycle system evaluation. To solve this problem, we propose a fuel-consumption simulation method for FCVs using a 1.2 kW stationary PEMFC (proton exchange membrane fuel cell). In this study, the specific fuel consumption under driving cycles such as the Japanese 10-15 and the JC08 modes are determined and compared with the FCV simulation results obtained using fuel consumption ratios derived from the stationary PEMFC. In the simulation, the specific fuel consumption was found to be 1.16 kg-H_2/100-km for the base case under the Japanese 10-15 driving cycle.

Key words: Proton exchange membrane fuel cell, fuel cell vehicle, fuel consumption, stationary, simulation.

1. Introduction

Environmental problems such as exhaustion of fossil fuels and GHG (greenhouse gas) emissions are associated with conventional diesel-powered and gasoline-powered automobiles. HEVs (hybrid electric vehicles), EVs (electric vehicles), and FCVs (fuel cell vehicles) have been developed to mitigate these problems. Having said that, HEVs also produce GHG emissions because they use fossil fuels, and EVs have a short range per charge, making both less than ideal solutions.

On the other hand, FCVs, being hydrogen-powered, do not produce any harmful emissions during their lifecycle [1]. Hydrogen can be abundantly obtained from various resources such as fossil fuels, biomass and water, and it is therefore considered a promising alternative fuel [2]. FCVs therefore represent the best solution to the abovementioned problems [3].

Corresponding author: Yutaro Akimoto, researcher, research fields: fuel cell, renewable energy and LCA. E-mail: r1220585@risk.tsukuba.ac.jp.

In an FCV, a FCS (fuel cell system) is used as a power source. An FCS comprises a PEMFC (proton exchange membrane fuel cell) and a battery. A PEMFC affords rapid startup, stable performance and easy operation in subzero temperatures, all of which are desirable for applications to vehicles [4]. Furthermore, the battery can be charged by the energy recovered during braking while the vehicle is running.

Manufacturers publish an FCV's specific fuel consumption, but not its dynamic characteristics such as fuel consumption ratio and motor power ratio. The fuel consumption ratio is the fuel consumption of each output power of fuel cell; it affects the specific fuel consumption. For calculating an FCV's specific fuel consumption, its fuel consumption over a unit distance and range should be known. However, studies have thus far reported only on the fuel consumption ratios in the steady state [5], manufacturer-published values [6], or theoretically determined values [7, 8]. Therefore, it is important to determine the dynamic characteristics of FCVs through a lifecycle evaluation for a

hydrogen-based driving environment. Although a large-scale social evaluation using actual FCVs is desirable, doing so would be difficult and inefficient.

To consider the effect of the dynamic characteristics on the specific fuel consumption, we propose a fuel consumption simulation method for FCVs powered by a 1.2 kW stationary PEMFC. In this study, the specific fuel consumptions in driving cycles such as the Japanese 10-15 and the JC08 modes are investigated and compared. Furthermore, the results of FCV simulation in the base cases are compared using the fuel consumption ratios derived from the stationary PEMFC.

2. Simulation Conditions

2.1 FCV Power Train

FCVs are of two types. In one type, the FCS is the only installed power source, and therefore, braking energy cannot be recovered. In the other type, called as FCHVs (fuel cell hybrid vehicles), a battery is installed as a power source in addition to the FCS, and therefore, braking energy can be recovered and used for charging the battery. An FCHV vehicle is driven through motors installed in each wheel that draw power from the FCS and the battery. In this study, we use an FCHV because its specific fuel consumption is better than that of FCVs. Table 1 lists the vehicle parameters and specifications of the power train used in this study [5]. This data was obtained from Ref. [9]. The FCV's power sources were a 45 kW FCS and a 1.5 kWh battery. The capacity and battery SOC (state of charge) are considered important parameters because they strongly influence the vehicle's range. The battery SOC is the ratio of the residual battery charge at a given instant to the full battery charge; in this study, it ranges from 0.3 to 0.7 [10]. The converters considered in this study are constant-efficiency ideal power converters.

2.2 Driving Cycle

A driving cycle is a series of data points representing the vehicle speed versus time. Many types of driving cycles are used worldwide. In Japan, the 10-15 mode is used most commonly. It was defined in 1992 for urban driving (10 mode) and suburban driving (15 mode). However, no improvements have been made to it recently with regard to the measurement technique and changes in driving environment. The JC08 mode, a new driving cycle, is also considered [11]. Fig. 1 shows the vehicle speed at each every second. There are differences in the maximum speed, average speed, cruising distance and measurement times. Therefore, the specific fuel consumption in the JC08 mode is less than that in the 10-15 mode. In this study, we simulated FCV driving in both modes.

Table 1 Vehicle parameters.

Item	Value
Vehicle total mass m	1,500 kg
Final drive gear efficiency η_g	0.95
Tire radius r	0.29 m
Aerodynamic drag coefficient Cd	0.37
Vehicle frontal area S	2.59 m^2
Air density ρ	1.21 kg/m^3
Rolling resistance coefficient μ_r	0.014
Elctric motor W_{max}	75 kW
FCS W_{FCmax}	45 kW
Battery	1.5 kWh
Efficiency of converters η_c	0.95

2.3 Experimental Apparatus

The experiment was carried out using a Nexa™ power module (Ballard Power Systems, Inc.). Fig. 2 shows the experimental apparatus. The Nexa™ power module is a small, fully automated FCS consisting of a stack and auxiliaries. It has a rated output of 1.2 kW. Hydrogen (> 99.99% purity) is supplied at the anode flow field with no humidification, and five psi pressure is maintained during rated operations using a regulator. Ambient air humidified through an in-built humidity exchanger is supplied to the cathode flow field. Air is removed from the outlet with an additional amount of water, while the hydrogen outlet is sealed. The stack is air-cooled through 18 vertical cooling holes between the cells.

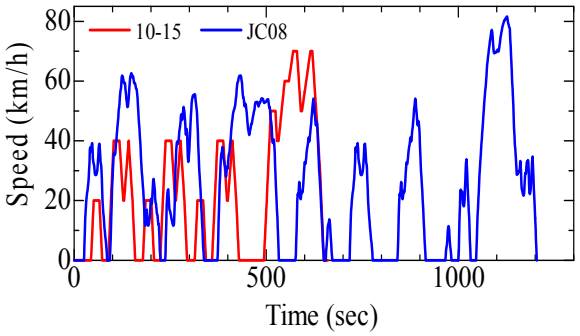

Fig. 1 Relationship between speed and time in each driving cycle.

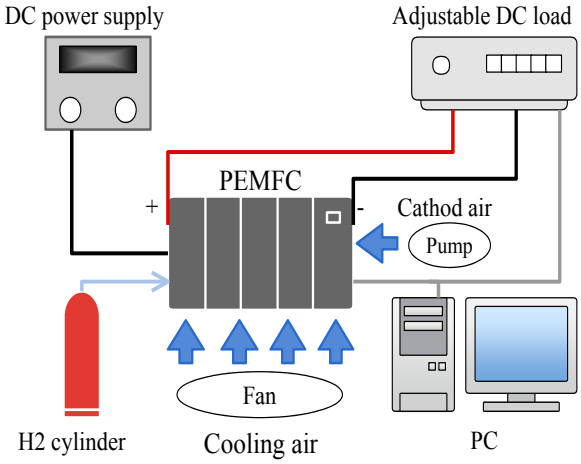

Fig. 2 Schematic diagram of experimental apparatus.

In the experiment, a 1 kW DC electric load (Takasago: FK–1,000 H) is used for loading the stack. The stack is operated at a variable power load of 0-1000 W, and the cell currents, voltages, and fuel consumption rate are measured using purpose-built monitoring software (Ballad Power System: NexaMon OEM2.0). A DC power supply (Kenwood: PA16-8A) is used for startup. All measurements were performed at ambient temperature.

Fig. 3 shows the performance of the PEMFC stack under constant power load operation. The open-circuit voltage is 42.12 V. The obtained output current and voltage obtained under a constant power load of 900 W are 32.34 A and 27.8 V, respectively. Fig. 4 shows the relationship between the fuel cell power and the fuel consumption under constant power load operation. The solid line indicates the fuel consumption ratio of the fuel cell in the steady state.

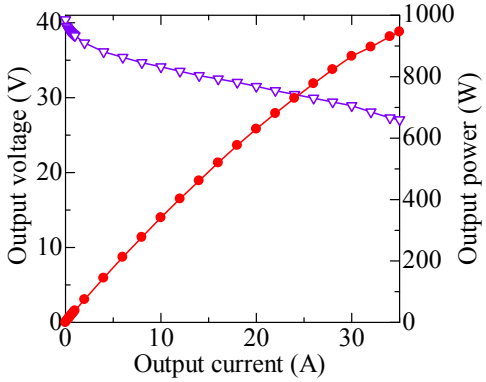

Fig. 3 PEMFC performance.

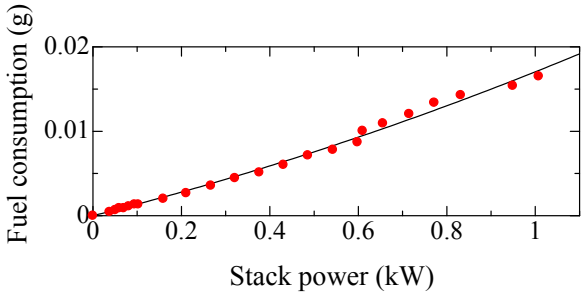

Fig. 4 Relationship between fuel cell power and fuel consumption.

3. Methods

3.1 Simulation Flowchart

Fig. 5 shows the simulation flowchart. In this study, the FCV driving simulation is carried out using a 1.2 kW stationary PEMFC under load following fuel cell operation.

Therefore, the stationary PEMFC's power is calculated using a scaled-down equation with regard to the car specifications, driving cycles, and FCS operation under rule-based management. The simulation results indicate the fuel consumption at the end of a driving cycle. This rate and the driving distance per driving cycle are used for calculating the specific fuel consumption.

3.2 FCS Operation

The driving simulation of the FCV with a battery is performed under FCS operation. The FCS operation performs fuel cell power management, which influences fuel consumption in a driving cycle. In this

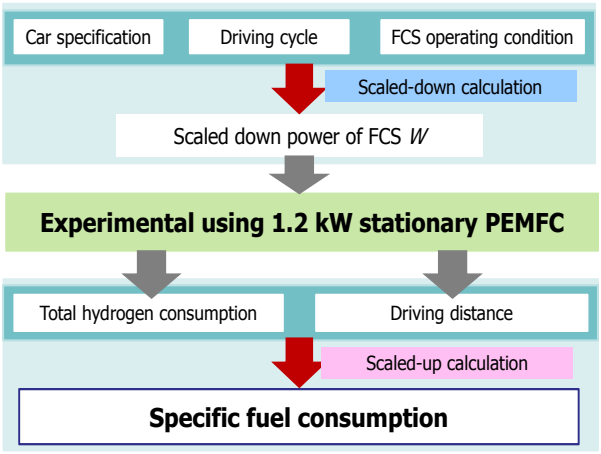

Fig. 5 Simulation flowchart.

study, the FCS operation adopts rule-based management. The operation is executed in four different modes, namely, battery mode, FCS mode, hybrid mode, and charge mode, as summarized in Table 2.

In the battery mode, the motor power W_m (kW) is supplied only by the battery because the FCS efficiency is low. The motor power is 0-5 kW, and the battery SOC is greater than 0.3 in this region, as follows:

$$\begin{aligned} W_m &= W_b \\ W_F &= 0 \end{aligned} \quad (1)$$

where, W_b (kW) denotes the battery power. In the FCS mode, the motor power is supplied only to the FCS, because its efficiency is high. The motor power exceeds 5 kW but is less than W_{cons} (kW), and the battery SOC is less than 0.3 in this region, as follows:

$$W_{\text{m}} = W_{\text{F}} \quad (2)$$

where, W_F (kW) denotes the FCS power and W_{cons}, the constant FCS power. W_{cons} affects fuel consumption. Thus, in this study, we use four different W_{cons} values for the four modes of operation: 10, 15, 20, and 25 kW. Furthermore, we define the base case as that in which W_{cons} is 20 kW.

In the hybrid mode, the FCV power is supplied to both the battery and the FCS. The motor power exceeds W_{cons} (kW), and the battery SOC is greater than 0.3 in this region, as follows:

$$\begin{aligned} W_m &= W_b + W_{cons} \\ W_F &= W_{cons} \end{aligned} \quad (3)$$

Table 2 FCS operation mode.

		Battery SOC		
		0-0.3	0.3-0.7	0.7-1.0
Motor power (kW)	-0	Charge mode	Charge mode	×
	0-5	FCS mode	Battery mode	Battery mode
	5-W_{cons}	FCS mode	FCS mode	FCS mode
	W_{cons}-	FCS mode	Hybrid mode	Hybrid mode

In the charge mode, braking energy is recovered and stored in the battery. The motor power is less than 0 W, and the battery SOC is less than 0.7 in this region, as follows:

$$\begin{aligned} Q_{bat} &= -W_m \eta_K \\ W_F &= 0 \end{aligned} \quad (4)$$

where, Q_{bat} (kW) denotes the battery SOC and η_g, the battery's recovery rate (= 0.74) [12]. If the SOC is greater than 0.7, braking energy is not recovered in order to prevent overcharging.

3.3 Conversion of Motor Power into FCS Power

In this study, the FCV driving simulation is performed using a 1.2 kW stationary PEMFC, as described in Section 2.3, under the load following operation of the fuel cell. Therefore, the power of the stationary PEMFC is calculated using the conversion equation with regard to the car specifications, driving cycles, and FCS operation under rule-based management. These parameters are used for calculating the driving power, vehicle running resistance, and motor power consumption rate. The driving power F (N) is calculated under the assumption that the vehicle running resistance R (N) is equal to the driving power, as follows [13]:

$$F = R = R_r + R_a + R_c \quad (5)$$

where, R_r, R_a, and R_c denote the rolling resistance, air resistance, and acceleration resistance, respectively. These factors are expressed as follows:

$$R_r = \mu_r mg \quad (6)$$

$$R_a = \frac{1}{2} C_d \rho S v^2 \quad (7)$$

$$R_c = (m + m')\alpha \quad (8)$$

In Eq. (6), μ_r denotes the rolling resistance; m, the total vehicle mass; and g (m/s^2), the gravitational acceleration (= 9.81). In Eq. (7), C_d denotes the aerodynamic drag coefficient; ρ (kg/m^2), the air density; S (m^2), the vehicle frontal area; and v (m/s), the vehicle velocity in the driving cycle. In Eq. (8), m' (kg) denotes the inertial mass and α (m/s^2), the acceleration rate in the driving cycle. Furthermore, the motor power W_m (kW) is expressed as follows:

$$W_m = \frac{2\pi rV}{\eta_c \eta_g} F \tag{9}$$

where, r (m) denotes the tire radius; V (m/s), the rolling velocity in the driving cycle; η_c, the converter efficiency; and η_g, the final drive gear efficiency. However, the FCS power W_F exceeds 1.2 kW because the FCS installed in the FCV is rated at 45 kW. Therefore, in this study, the scaled down power of W (kW) is calculated using the conversion equation considering the motor power consumption of a 1.2 kW stationary PEMFC, as follows:

$$k = \frac{W_{FCS}}{W_0} \tag{10}$$

$$W = \frac{W_F}{k} \tag{11}$$

where, W_{FCS} (kW) denotes the maximum FCS power and W_0 (kW), the stationary PEMFC maximum power.

3.4 Calculation of Specific Fuel Consumption

In this experiment, the scaled-down power W is input to a DC electrical load connected to the stationary PEMFC every second. The input power range of the DC electrical load employed herein is 40 -1,000 W. Therefore, the scaled-down power W is 40 W; when this value is less than 40 W, we define it as the FCS's idling state.

At the end of a driving cycle, specific monitoring software is used for obtaining output parameters such as stack currents, voltages and hydrogen consumption rate. The specific fuel consumption is expressed as follows:

$$FE_{FCV} = \frac{100}{d} kL \tag{12}$$

where, FE_{FCV} (kg-H_2/100-km) denotes the specific fuel consumption; L (kg), the total hydrogen consumption in this experiment; and d (km), the driving distance.

4. Results and Discussion

4.1 Experimental Result

The FCS powers are calculated using Eqs. (1)-(9) and the vehicle parameter values. The maximm FCS power values obtained in the Japanese 10-15 and the JC08 modes are 23.6 kW and 25.7 kW, respectively. The scaled-down power W in this experiment is calculated using Eqs. (10) and (11). Fig. 6 shows the output power of the 1.2 kW PEMFC in the base case, which is not greater than 444 W. In this manner, the 1.2 kW of the PEMFC is generated under the load following operation in the constant-power mode. In this experiment, the PEMFC stack power was not less than the scaled-down power W and showed sufficient response to the input value.

4.2 Fuel Consumption in 10-15 and JC08 Modes

Fig. 7 shows the specific fuel consumption values in the Japanese 10-15 and the JC08 modes. In this study, the battery is assumed to be fully charged initially; thus, the SOC starts from 0.7 for the driving cycles.

For the base case wherein W_{cons} is 20 kW under the Japanese 10-15 and the JC08 modes, the specific fuel consumption values were 1.15 kg-H_2/100-km and 1.16 kg-H_2/100-km, respectively. In other words, the specific fuel consumption under the Japanese JC08 driving cycle was 0.56% higher. The reported specific consumption under the Japanese 10-15 mode [5] is 1.09 kg-H_2/100-km. It is less than that in this study, because the reported one was considered as zero under no output from the motor. In this study, however, the FCS consumes fuel in the idling state when the input value of W is less than 40 W.

Fig. 8 shows that the final SOC values under the Japanese 10-15 and the JC08 modes were 0.65 and 0.64, respectively; the JC08 mode value is lower because the distance driven in that mode is longer. When W_{cons} is

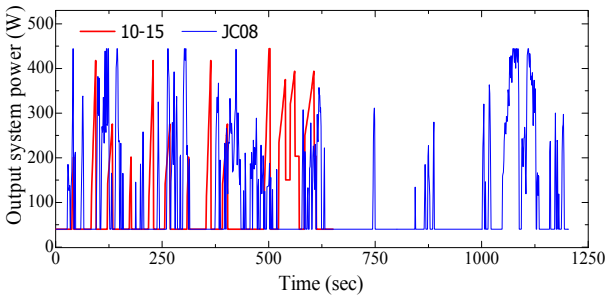

Fig. 6 Output power of 1.2 kW PEMFC in base case.

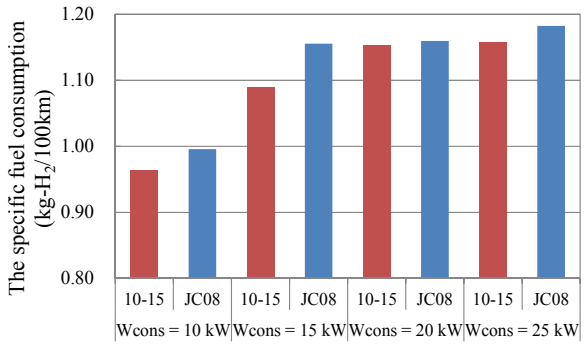

Fig. 7 Specific fuel consumption in Japanese 10-15 and JC08 modes.

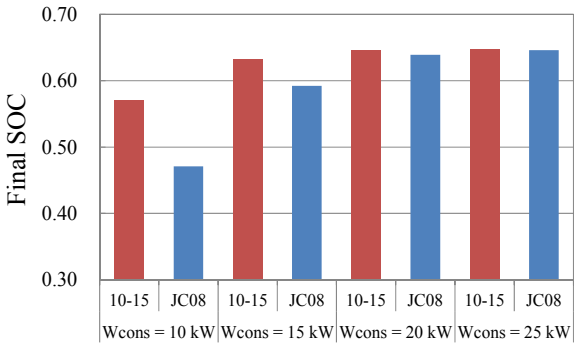

Fig. 8 Final SOC in Japanese 10-15 and JC08 modes.

lower than 20 kW, the specific fuel consumption is low because battery power is consumed instead of FCS power. Therefore, the final SOC was less than that in the base case.

Fig. 9 shows the rate of motor power under the Japanese 10-15 and the JC08 modes. The FCS power is 0-5 kW or more than 70% of the measurement time. Because the vehicle is in the FCS or hybrid mode for the remaining measurement time, it affects the specific fuel consumption and the final SOC. When W_m exceeds 20 kW, the rate of motor power under the Japanese 10-15 mode was 0.5%. Thus, the specific fuel

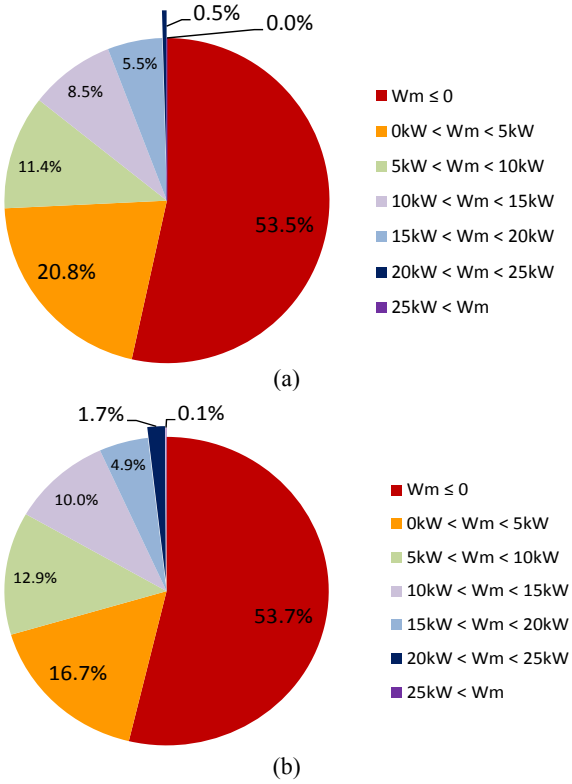

Fig. 9 (a) Motor power rate in Japanese 10-15 mode; (b) motor power rate in JC08 mode.

consumption and the final SOC differ little from the result of the base case. However, the specific fuel consumption under the Japanese JC08 mode was greater than that in the base case because the rate of motor power was 1.8%, which is higher than that under the Japanese 10-15 mode.

4.3 Comparison of Specific Fuel Consumption

In a previous research [5], the fuel consumption ratios in the steady state were used for calculating the specific fuel consumption. Thus, the specific fuel consumptions in the base case in the Japanese 10-15 and the JC08 modes are compared with the calculation results arrived at using the fuel consumption ratios in the steady state obtained from the stationary PEMFC.

Fig. 10 shows the specific fuel consumption yielded by the proposed simulation model used in this study and the calculated values using the fuel consumption ratios derived from the stationary PEMFC. The specific fuel consumptions obtained using the fuel consumption ratios in the steady state under the Japanese 10-15 and the JC08

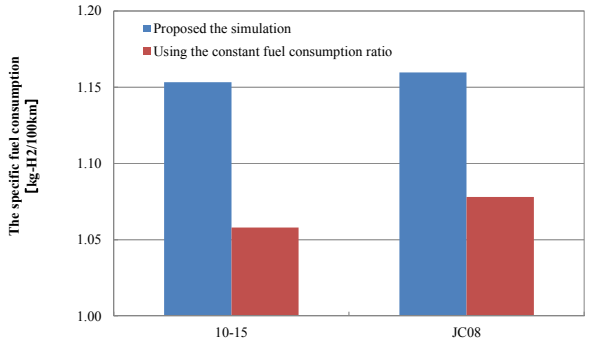

Fig. 10 Comparison of specific fuel consumption in base case.

modes are 1.06 kg-H_2/100-km and 1.08 kg-H_2/100-km, respectively. These consumptions are lower than the results of the proposed simulation method.

Fig. 11 shows the dynamic behaviors of fuel consumption in the proposed simulation model. There is a similar tendency between the fuel consumption ratio of the FCS in the Japanese 10-15 and the JC08 modes. Variability in the 5-10 kW range is 0.04 -0.28 g. A large difference is observed at an FCS power of 0 kW owing to the power consumption by the auxiliaries.

The median and standard deviation are calculated for four FCS power bins, namely, 0-5, 5-10, 10-15 and 15-20 kW. Fig. 12 shows the median of fuel consumption for each bin. When the FCS power is 0 kW, the specific fuel consumption is greater than that obtained using fuel consumption ratios derived from the stationary PEMFC. The state in which the FCS power is 0-5 kW occupies more than 70% of the measurement time, as shown in Fig. 9. Thus, the increase in the specific fuel consumption in this simulation is attributed to the fuel consumed by FCS idling.

Fig. 13 shows the standard deviation of the fuel consumption observed from the experimental results. In this simulation, the fuel consumption varies widely, but the minimum standard deviation is 0.02 and the maximum is 0.04. These values are very small and are virtually constant.

5. Conclusions

In this study, a simulation model for determining the

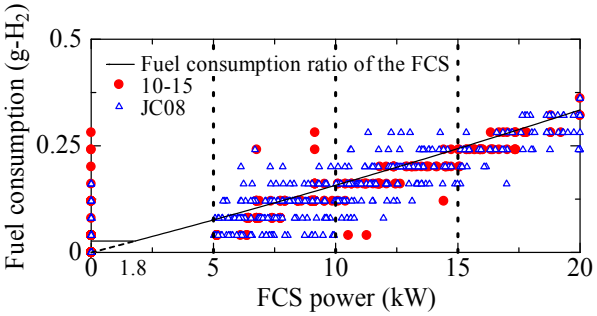

Fig. 11 Distribution of the fuel consumption.

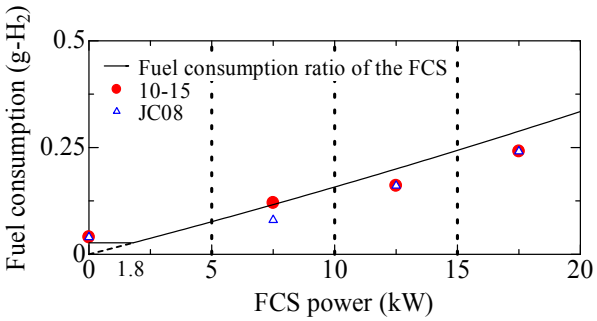

Fig. 12 Median of the fuel consumption.

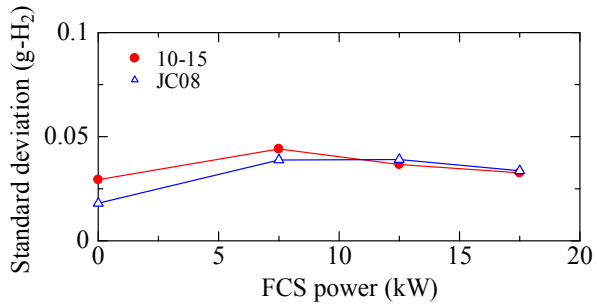

Fig. 13 Standard deviation of the fuel consumption.

specific fuel consumption of an FCV using a stationary PEMFC was proposed and evaluated. The specific fuel consumptions for driving cycles in four different modes were investigated and compared with the FCV simulation results using the fuel consumption ratios derived from the stationary PEMFC in the base case.

The specific fuel consumption values under the Japanese 10-15 and the JC08 modes are 1.153 kg-H_2/100-km and 1.160 kg-H_2/100-km, respectively, in the base case. When W_{cons} is lower than 20 kW, the specific fuel consumption is low because battery power is consumed instead of FCS power. Therefore, the final SOC is less than that in the base case. When W_{cons} is higher than 20 kW, the motor power rate under the

Japanese 10-15 mode is 0.5%. Thus, the specific fuel consumption differs slightly from that in the base case.

The base case results are compared with the FCV simulation results using the fuel consumption ratios derived from the stationary PEMFC. In the Japanese 10-15 and JC08 modes, the specific fuel consumption values obtained using the steady-state fuel consumption ratios are 1.06 kg-H_2/100-km and 1.08 kg-H_2/100-km, respectively. These values are smaller than those obtained from the results of the proposed simulation method because the fuel consumption in actual systems is not constant in terms of the FCS power. Although this simulation precisely measures the specific fuel consumption, it can be used for determining the effect of dynamic characteristics such as variability in fuel consumption. Therefore, this method can provide independent and objective information on the real-world specific fuel consumption of FCVs.

Conflict of Interests

The authors declare that there is no conflict of interests regarding the publication of this article.

Acknowledgements

This work was supported by JSPS KAKENHI Grant Number 24360403.

References

[1] The Energy Policy Act, U.S. Department of Energy, 1992.

[2] ANL, Fuel choices for fuel cell vehicles: Well-to-wheels energy and emission impacts, J. Power Sources 112 (1) (2002) 307-321.

[3] Fuel Cell Electric Vehicles, USDOE Web site, 2013, http://www.afdc.energy.gov/vehicles/fuel_cell.html.

[4] Y. Wang, K.S. Chen, J. Mishler, S.C. Cho, X.C. Adroher, A review of polymer electrolyte membrane fuel cells: Technology, applications, and needs on fundamental research, J. Applied Energy 88 (2011) 981-1007.

[5] C.H. Zheng, C.E. Oh, Y.I. Park, S.W. Cha, Fuel economy evaluation of fuel cell hybrid vehicles based on equivalent fuel consumption, J. Hydrogen Energy 37 (2012) 1790-1796.

[6] J.J. Hwang. Sustainability study of hydrogen pathways for fuel cell vehicle applications, Renewable and Sustainable Energy Reviews 19 (2013) 220-229.

[7] J.J. Hwang, J.K. Kuo, W. Wu, W.R. Chang, C.H. Lin, S.E. Wang, Lifecycle performance assessment of fuel cell/battery electric vehicles, J. Hydrogen Energy 38 (2013) 3433-3446.

[8] X.P. Li, J.M. Ogden, Understanding the design and economics of distributed tri-generation systems for home and neighborhood refueling-part1: Single family residence case studies, J. Power Sources 196 (2011) 2098-108.

[9] J. Bernard, S. Delprat, F. Buechi, T.M. Guerra, Fuel-cell hybrid power train: Toward minimization of hydrogen consumption, IEEE Trans Vehicular Technology 58 (7) (2009) 3168-3176.

[10] Battery RM 2008, New Energy and Industrial Technology Development Organization, 2008.

[11] From 10-15 to JC08: Japan's New Economy Formula, JAMA [Online], 2013, http://www.jama-english.jp/europe/news/2009/no_2/peternunn.html.

[12] M. Yasushi, Y. Fukuda, S. Ohsawa, K. Fujii, A car navigation system that shows the driving range of an electric vehicle, PIONEER R & D 20 (1) (2011) 1-7. (in Japanese)

[13] S. Hiroshi, All of the Electric Vehicles, Nikkan Kogyo Shimbun, Japan, 1998. (in Japanese)